KSS-10/Hdq

NASA CR - 112233

A PARAMETRIC STUDY OF PLANFORM AND AEROELASTIC EFFECTS ON AERODYNAMIC CENTER, α- AND q- STABILITY DERIVATIVES

APPENDIX E

PROCEDURES USED TO DETERMINE THE STRUCTURAL REPRESENTATION FOR IDEALIZED LOW ASPECT RATIO TWO SPAR FIGHTER WINGS

by

J. Roskam, C. Lan, H. Smith, and G. Gibson

CRINC-FRL 72-015

October 1972

Prepared under NASA Grant NGR 17-002-071 by

The Flight Research Laboratory

Department of Aerospace Engineering

The University of Kansas

Lawrence, Kansas 66044

for

Langley Research Center

National Aeronautics and Space Administration

TABLE OF CONTENTS

1. INTRODUCTION

Before it is feasible to compute a structural influence coefficient matrix with the method of Reference 1 (Appendix B of the Summary Report), the structural properties of the wing must be established. In this appendix, an explanation is presented of the method used to locate the elastic axis and the method to determine the EI and GJ distributions along the elastic axes of the wings of the parametric study of Reference 2. The method applies exclusively to wings with a 2-spar (front and rear) construction or a single torque-box construction.

2. SYMBOLS

The units used for the physical quantities defined in this paper are given both in the International System of Units (SI) and the U.S. Customary Units.

Symbols	Definition	Dimension
AR	Aspect ratio	
b	Wing span	ft (m)
$\bar{c}$	Average chord	in (m)
c_r	Root chord	ft (m)
c_s	Structural root chord	in (m)
E	Modulus of elasticity	lb/in^2 (N/m^2)
EI	Bending stiffness	$lb\text{-}in^2$ $(N\text{-}m^2)$
G	Shear modulus, Flexural stress	lb/in^2 (N/m^2)
GJ	Torsional stiffness	$lb\text{-}in^2 (N\text{-}m^2)$
I	Section moment of inertia	$in^4 (m^4)$
k	Constant thickness ratio	
ℓ	Length	in (m)
M	Bending moment	in-lb (m-N)
S	Wing reference area	$ft^2 (m^2)$
t/c	Thickness ratio	
w	Load per unit length of span	lb/in (N/m)
W	Total airplane weight	lb (N)
λ	Taper ratio	
$\Lambda_{c/4}$	Quarter-chord sweep angle	deg
Λ_{LE}	Leading-edge sweep angle	deg

3. METHOD USED TO LOCATE THE ELASTIC AXIS ON TWO-SPAR PLANFORMS

Before the elastic axis can be located, it is necessary to determine where in the planform the front and rear spars are located. The result is a planform sketch as shown in Figure 1. For typical fighter wings it is reasonable to assume that the elastic axis starts perpendicular to the center line and gradually bends toward a straight line located half-way between the two spars. This is also shown in Figure 1. Location of points A and B depends on the planform sweep angle.

Figure 2 shows the ground rules for locating points A and B of the elastic axis for two-spar planforms. Figure 2a locates the elastic axis at the centerline of the planform (i.e., point A), and Figure 2b locates the fraction of the semispan at which the elastic axis becomes straight (i.e., point B).

All the fixed-sweep planforms used (Wings 1, 5 and 7) in the investigation of Reference [2] had their elastic axis located according to the method of Figures 1 and 2. The planforms with pivots located at 20%, 30%, and 40% half-span (Wings 2, 3, 4, 9, 10, and 11 of Reference 2) had their elastic axis position assumed. For the latter planforms, the elastic axis was assumed to be straight and located midway between the spars from the outboard end of the strake to the wing tip. An example is shown in Figure 3. In the region of the strake, the elastic axis was assumed to be a straight line from the planform centerline to the pivot, and again a straight line from the pivot to the inboard 50% chord location at the outboard end of the strake, see Figure 3.

The two planforms with cranked tips (Wings 6 and 8 of Reference 2) had their elastic axis located per Figure 2 until the cranked position was reached. At the cranked position the elastic axis was assumed to be positioned mid-way between the spars, and vary linearly outboard to the wing tip, see Figure 4.

4. METHOD USED TO ESTABLISH EI AND GJ VALUES FOR TWO-SPAR PLANFORMS

A typical bending and torsional stiffness (EI and GJ respectively) distribution for fighter-type wings is presented in Figure 5. It should be emphasized that the distributions of Figure 5 apply only to fighter aircraft with a weight of approximately 40,000 lbs and a design limit load factor of 7.33. Bending and torsional stiffness distributions similar to that of Figure 5 were generated for all planforms used in the investigation of Reference 1.

In using Figure 5 to generate EI and GJ plots for different planforms, the stress at any point in the new planform must be equal to the stress at corresponding points in the planform represented by Figure 5. Development of an expression relating the stress between two planforms requires the following assumptions:

1) Stress at any point on the test planform equals the stress at a corresponding point on the planform of Figure 5.

2) Thickness ratio (t/c) equals a constant k.

3) The two wings are made of the same materials. Thus the modulus of elasticity (E) and the shear modulus (G) are the same in both wings.

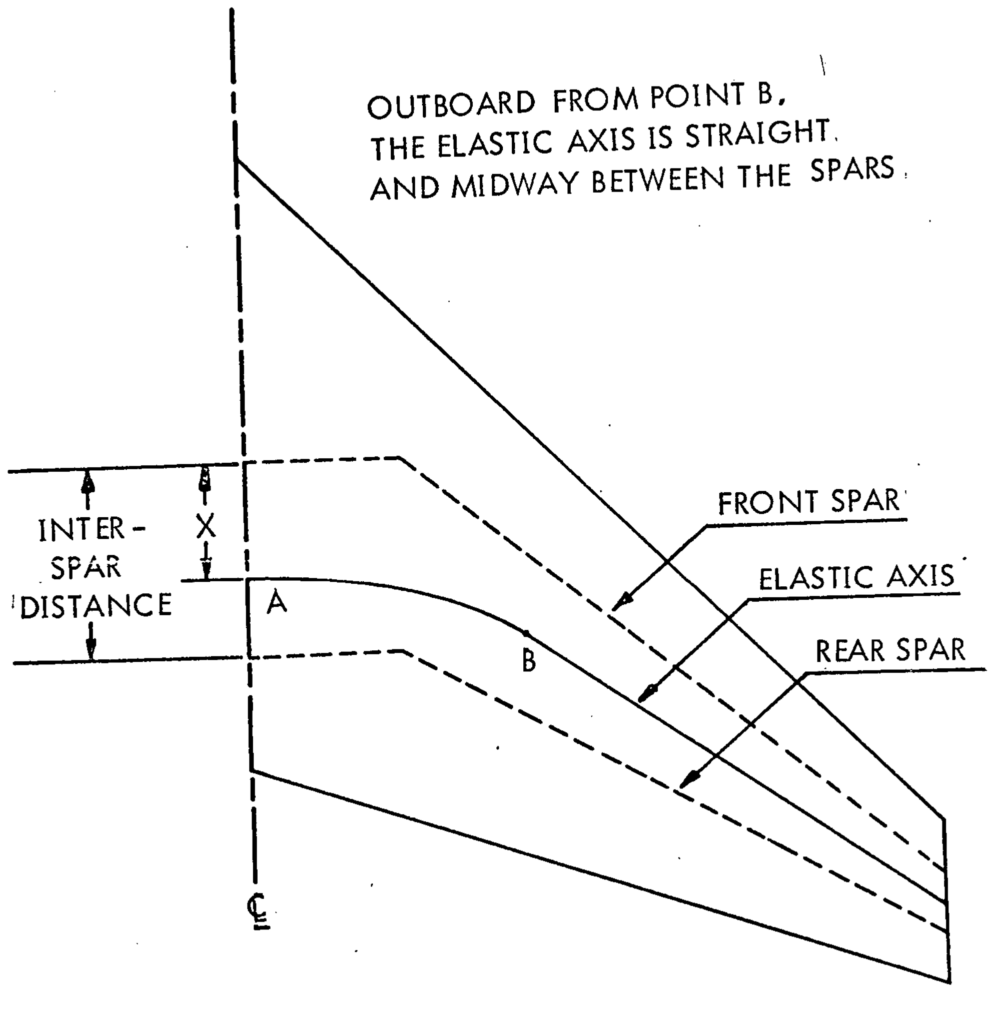

Figure 1 Planform Sketch Including Spar Locations

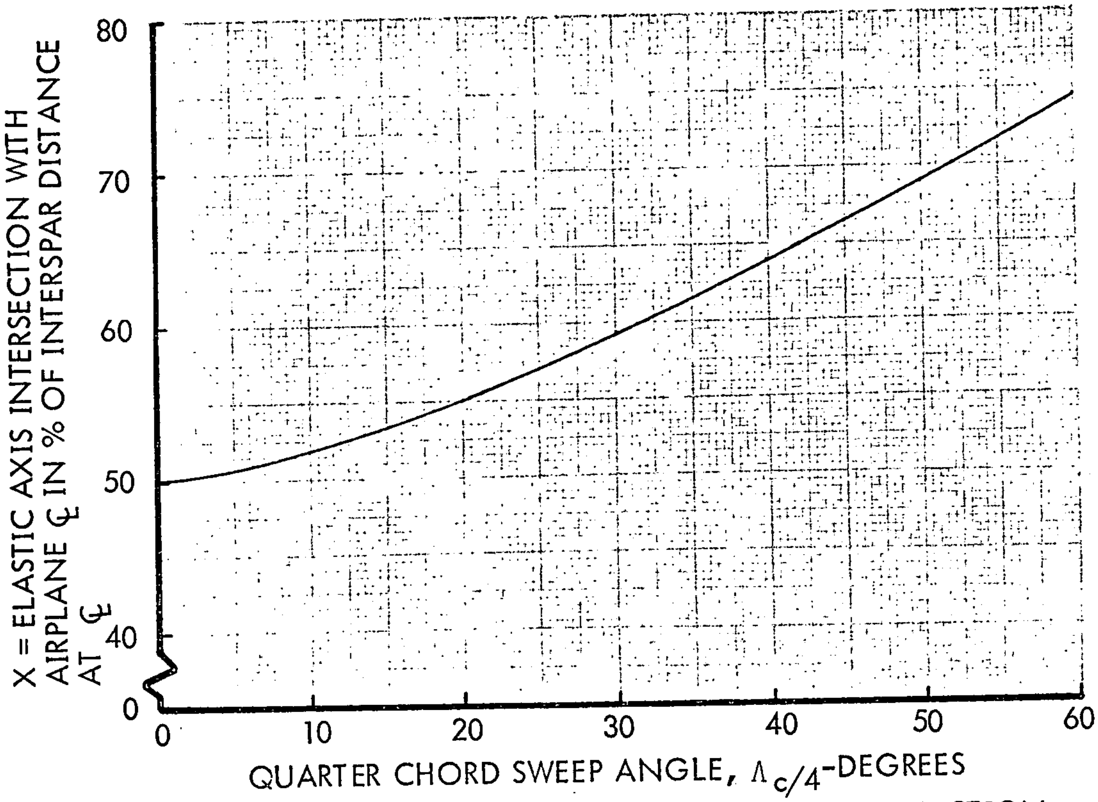

a) DETERMINATION OF ELASTIC AXIS INTERSECTION IN THE WING CENTERLINE

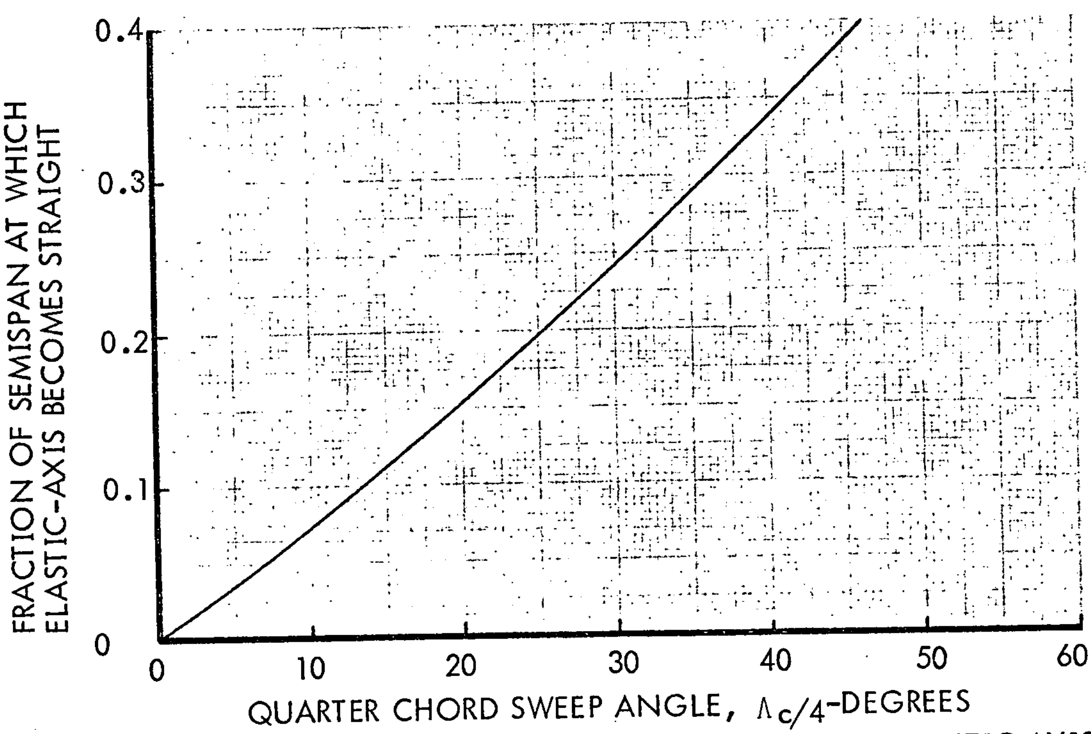

b) DETERMINATION OF POINT WHERE THE ELASTIC AXIS BECOMES STRAIGHT

Figure 2. Ground Rules for Elastic Axis Location

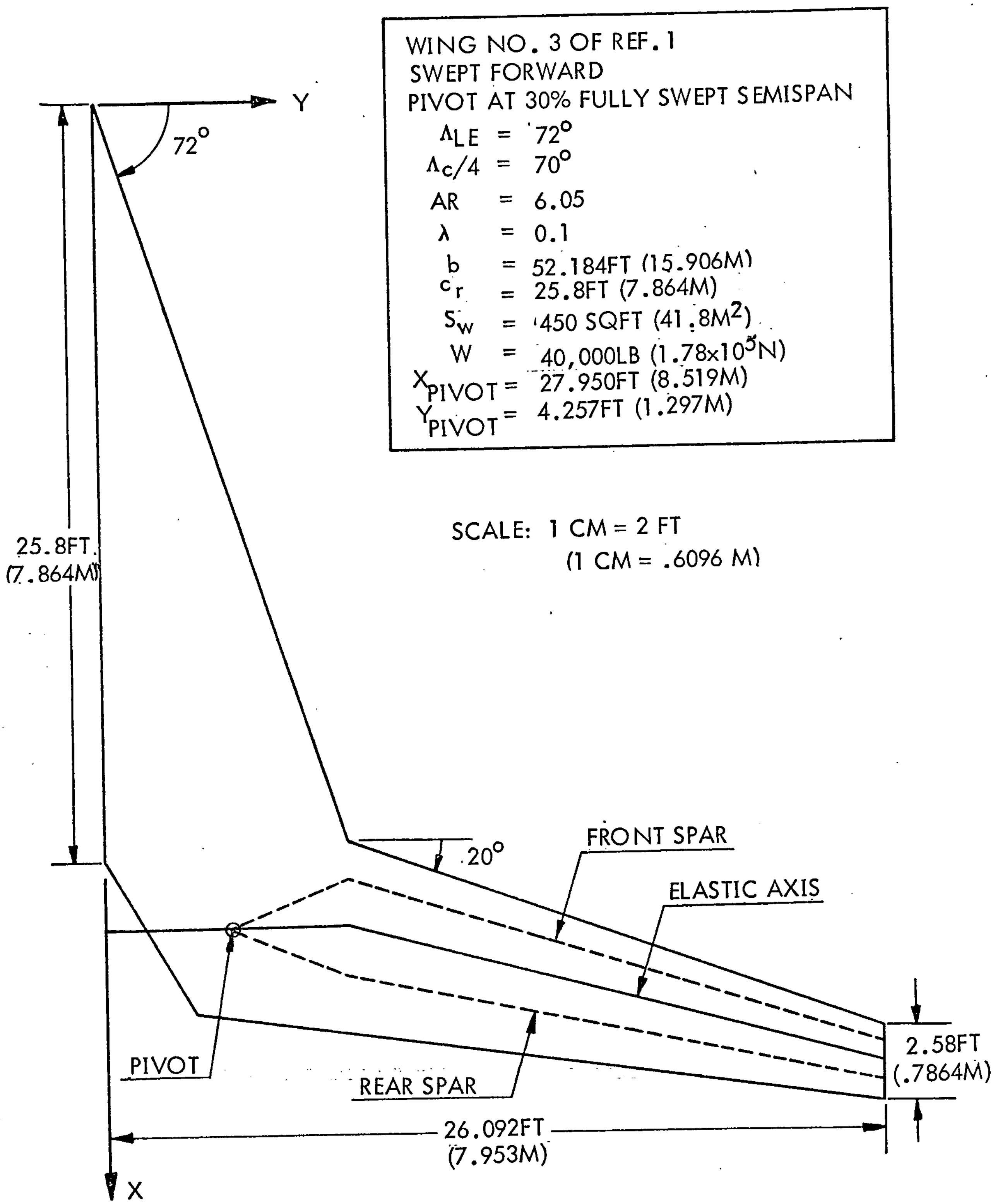

Figure 3 Elastic Axis Location for a Variable Sweep Wing

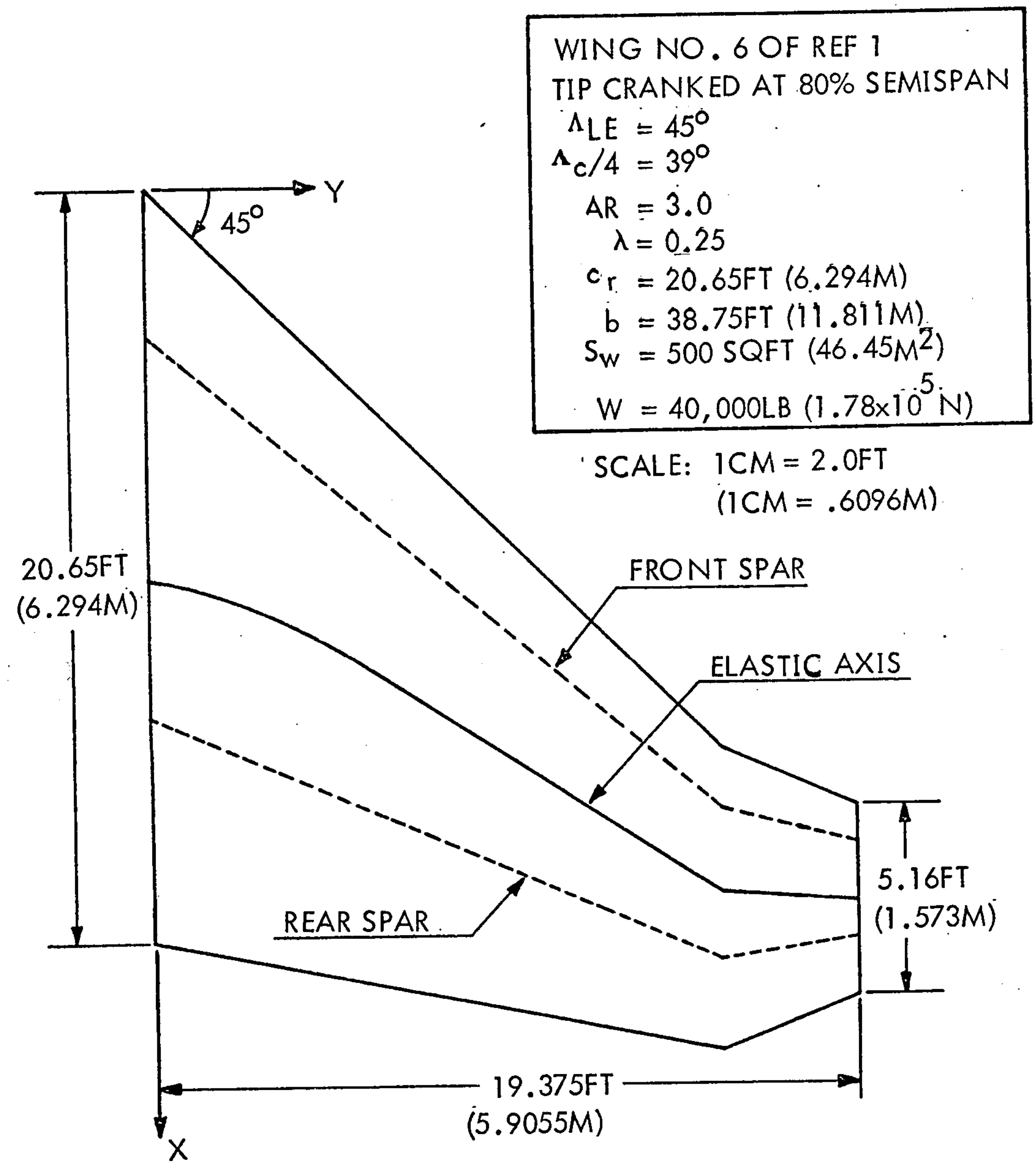

Figure 4 Elastic Axis Location for Wings with Cranked Tips

With these assumptions, the stress relationship is derived using the flexural stress equation:

$$\sigma = \frac{My}{I} \tag{1}$$

where σ is the flexural stress, M the bending moment, y the distance between the neutral axis and the outer most fiber of a section and I the section moment of inertia.

For a cantilever beam with a uniform load,

$$M = \frac{w\ell^2}{2} \tag{2}$$

and

$$w = \frac{W\bar{c}}{S} \tag{3}$$

where w is the load per unit length of span and $\bar{c}$ the average chord. The expression for the moment becomes:

$$M = \frac{Wb^2\bar{c}}{8S} \quad . \tag{4}$$

Letting "y", from the flexure formula, equal 1/2 "t" from the thickness ratio, the expression for the thickness ratio becomes:

$$2y/c = k \quad . \tag{5}$$

Letting $c = c_s$, the root chord, and dividing both sides of the equation by 2, it follows that:

$$y = \frac{kc_s}{2} \quad . \tag{6}$$

Substituting the expressions for "M" and "y" into the flexure formula, the flexural stress is given by:

$$\sigma = \frac{Wb^2\bar{c}k\,c_s}{16SI} \quad . \tag{7}$$

Equating the stress expressions, it is found that:

$$\sigma_A = \frac{W_A b_A^2 \bar{c}_A k c_{s_A}}{16 S_A I_A} = \sigma_B = \frac{W_B b_B^2 \bar{c}_B k c_{s_B}}{16 S_B I_B} \quad . \tag{8}$$

From this relation:

$$EI_B = \frac{(W/S)_B b_B^2 \bar{c}_B c_{s_B}}{(W/S)_A b_A^2 \bar{c}_A c_{s_A}} EI_A \quad . \tag{9}$$

Equation (9) was used to generate the bending stiffness for the planforms of the parametric study reported in Reference 2.

Due to the complexity of the stress formulas for unsymmetric sections, a linear re-

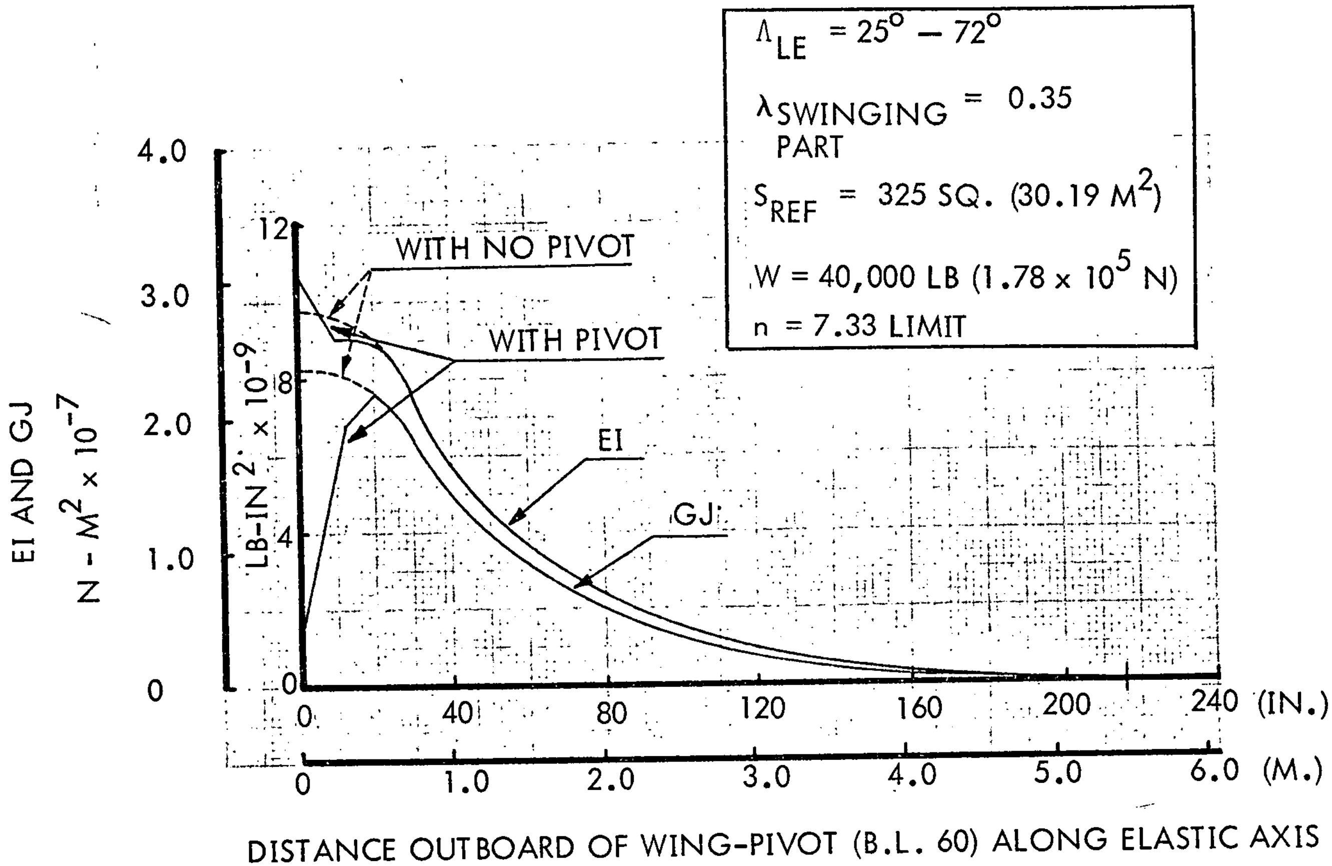

FIGURE 5. Typical Fighter EI and GJ Distributions

lationship was assumed between the EI and GJ values of planforms "A" and "B." Thus a ratio was established as follows:

Let EI_B be the bending stiffness calculated by Equation (9). Let EI_A and GJ_A be bending and torsional stiffness values corresponding to Figure 5. For each point on the span represented by Figure 5, new GJ_B values can be calculated for the study planform by using the following ratio:

$$GJ_B = \left(\frac{EI_B}{EI_A}\right) GJ_A \tag{10}$$

This result indicates that the torsional stiffness is increased by the same percentage that the bending stiffness is increased.

The procedure outlined before was used to find the EI and GJ distributions for all the planforms used in the investigations of Reference 2. A typical plot for a wing without pivots is given in Figure 6.

5. METHOD OF DETERMINING INPUT DATA FOR THE STRUCTURAL INFLUENCE COEFFICIENT SUBROUTINE

The data used as inputs to the structural program consist of the following:

1) Coordinates of the end points of the elastic axis segments.
2) Bending and torsional stiffness, (EI and GJ respectively), for each segment of the elastic axis.
3) Assignment of aerodynamic panels to specific end points of the elastic axis segments.

First of all, the elastic axis is broken at the centerline of each chordwise column of panels, the pivot point and the outboard end of the strake (point A), as shown in Figure 7. Knowing the end points of each segment, their respective coordinates can be found, since the elastic axis location is known and the y-coordinate of the centerline of each chordwise column of panels can be obtained from the aerodynamic program described in Reference 3 (Appendix C of the Summary Report).

Once the coordinates of the elastic axis segments are known, the bending and torsional stiffness for each segment can be found with the following procedure. First, locate the end points of each segment on the corresponding stiffness plot, Figure 8. Then select numerous points between and including the endpoints of each segment. For each selected point read EI and GJ values and take their respective averages. These EI and GJ averages represent the EI and GJ values for each segment. Table 1 shows the result of this method applied to the planform of Figure 7.

The last data needed as inputs to the structural influence coefficient subroutine are the elements of the vector matrix IASIGN. The matrix IASIGN is used to assign aerodynamic panels to specific end points of the elastic axis (see also Reference 1). In general, a panel is assigned to a segment of the elastic axis in a direction perpendicular to the elastic axis and is assumed attached to the outboard endpoint of the assigned segment. See Figures 9 and 10. The panel located below the pivot is assigned to the pivot. The results of application of this procedure to the wing in Figure 7 are listed in Table 2.

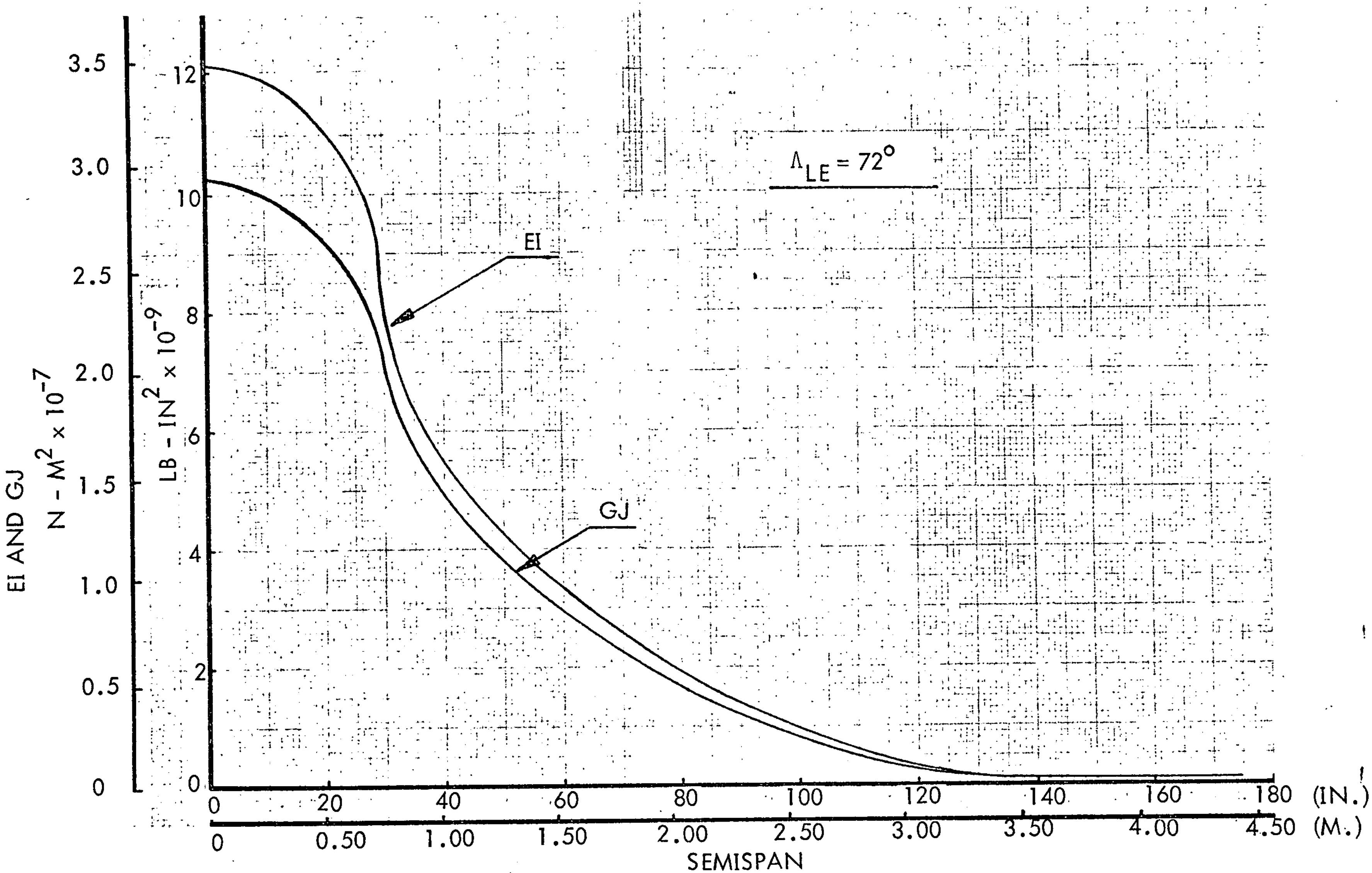

Figure 6. EI and GJ Distributions for a Wing Without Pivot

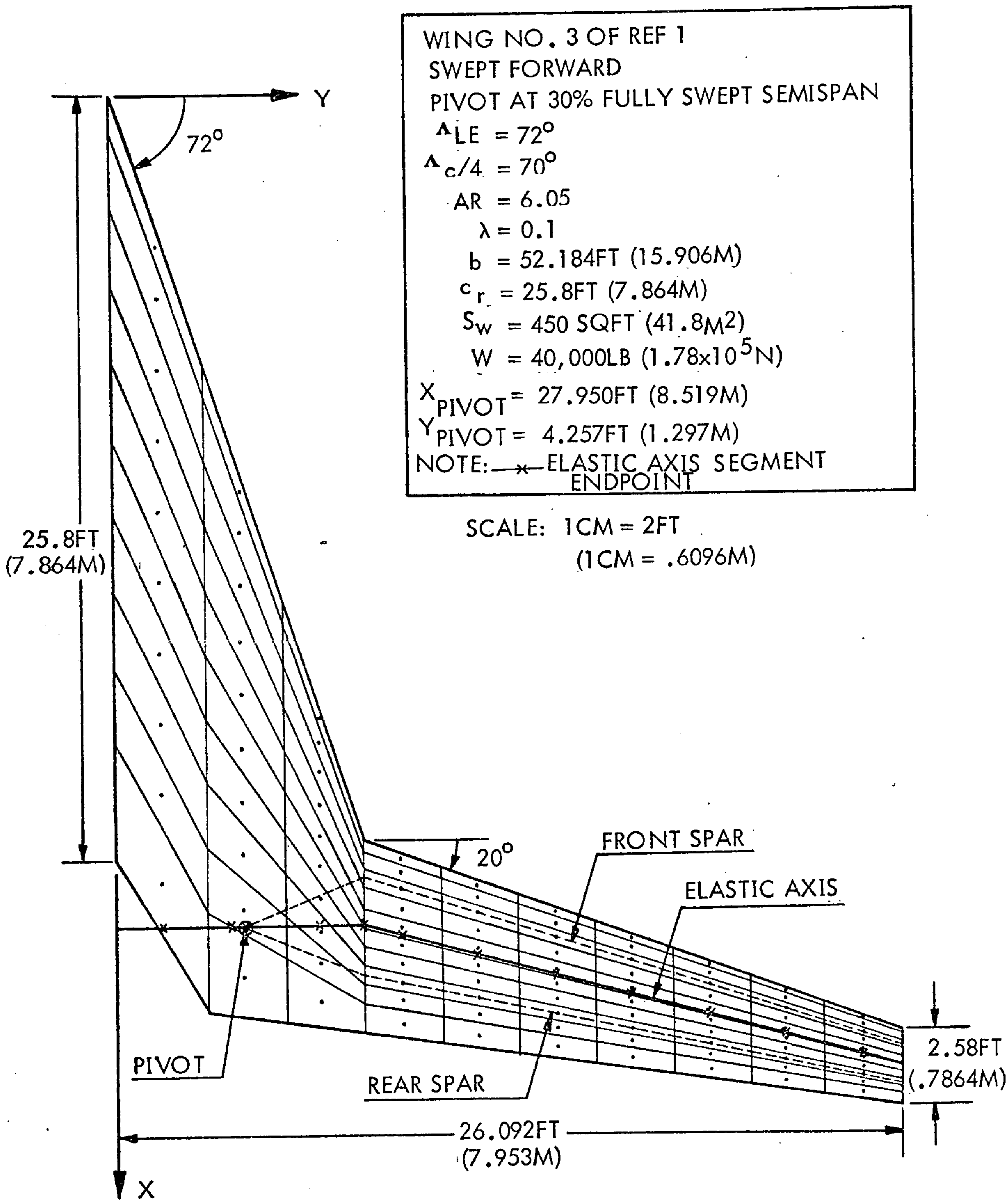

Figure 7 Example of Elastic Axis Segments

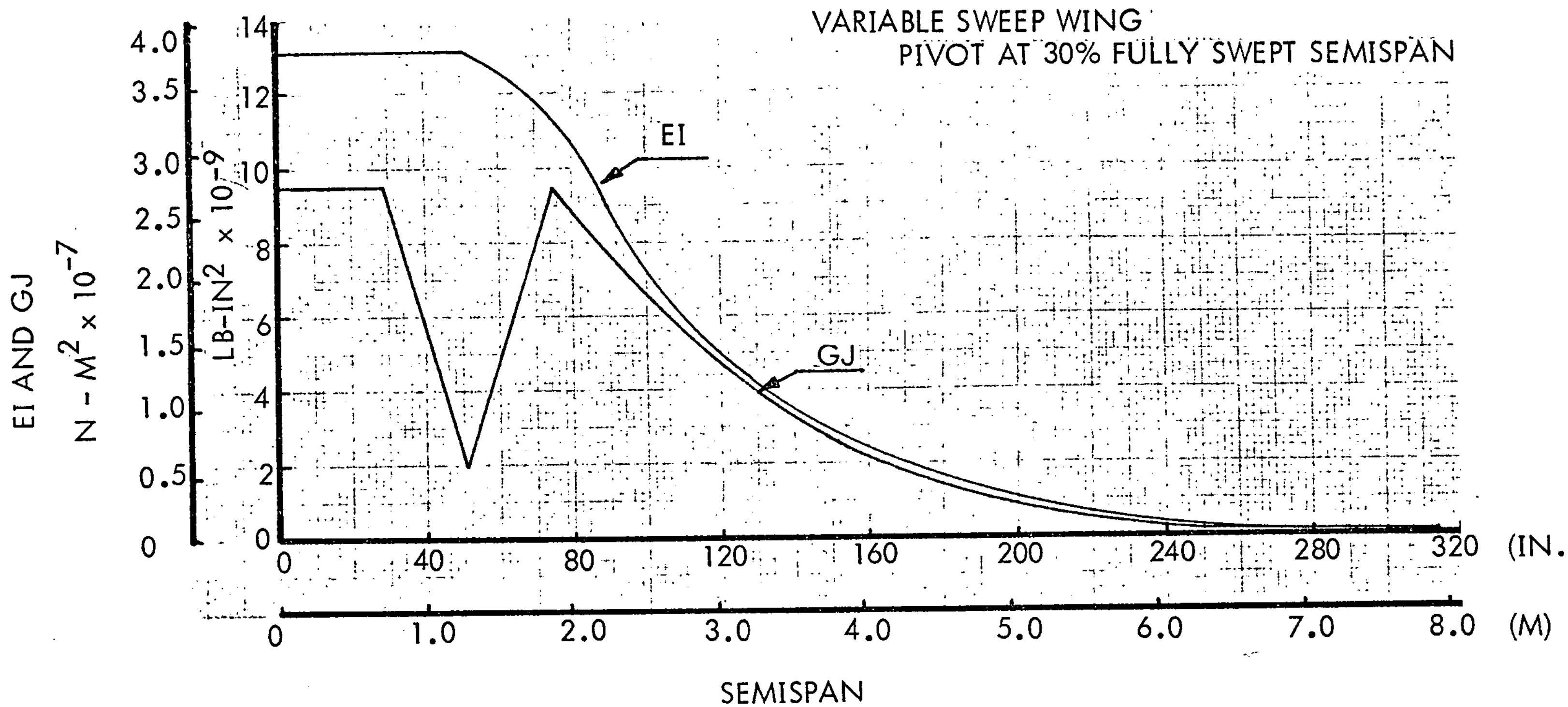

Figure 8. EI and GJ Distributions for the Example Wing (Swept Forward)

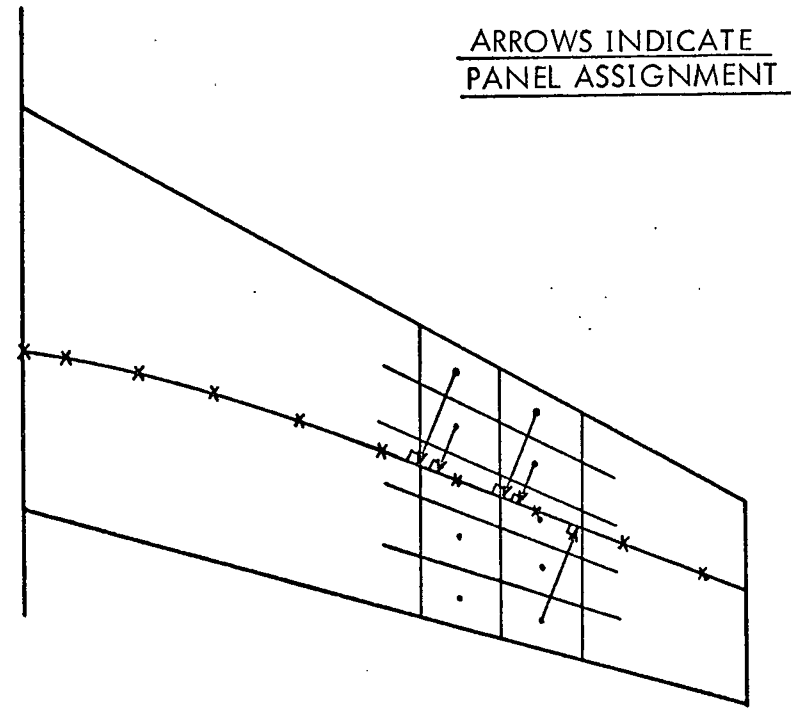

Figure 9 Examples of Panel Assignment to the Elastic Axis

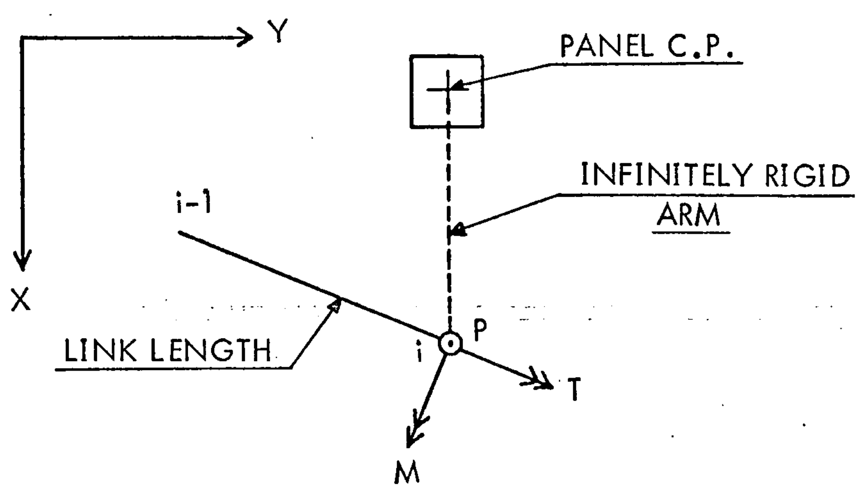

Figure 10 Panel Connection to Elastic Axis Link Length and Positive Loading Condition

Table 1. EI and GJ Values for the Example Wing of Figure 7

SEGMENT	EI $lb\text{-}in^2 \times 10^{-9}$	EI $N\text{-}m^2 \times 10^{-6}$	GJ $lb\text{-}in^2 \times 10^{-9}$	GJ $N\text{-}m^2 \times 10^{-6}$
1-2	13.19	37.9	9.59	27.6
2-3	13.19	37.9	7.63	21.6
3-4	13.19	37.9	2.75	7.90
4-5	11.80	33.9	6.10	17.5
5-6	9.10	26.1	7.59	21.8
6-7	6.50	18.65	6.05	17.36
7-8	4.45	12.78	4.00	11.48
8-9	2.55	7.32	2.29	6.58
9-10	1.45	4.17	1.20	3.44
10-11	0.66	1.894	0.55	1.578
11-12	0.13	0.373	0.085	0.244
12-13	0.060	0.172	0.047	0.135

Table 2. Elements of Matrix "IASIGN" for the Example Wing of Figure 7.

PANELS	ASSIGNED TO ELASTIC AXIS POINT NO.
1-10	2
11-19	3
20	4 PIVOT
21-27	5
28-30	6
31-35	7
36-45	8
46-55	9
56-65	10
66-75	11
76-85	12
86-100	13

6. REFERENCES

1. Roskam, J., Smith, H., and Gibson, G.; "Method for Computing the Structural Influence Coefficient Matrix of Nonplanar Wing-Body-Tail Configurations," NASA CR-12230; Prepared under NASA Grant NGR 17-002-071 by the Flight Research Laboratory of the Department of Aerospace Engineering of the University of Kansas, October, 1972. Appendix B of the Summary Report, NASA CR-2117.

2. Roskam, J., and Lan, C.; A Parametric Study of Planform and Aeroelastic Effects on Aerodynamic Center, - and q- Stability Derivatives; NASA CR-2117, Summary Report; Prepared under NASA Grant NGR 17-002-071 by the Flight Research Laboratory of the Department of Aerospace Engineering of The University of Kansas, October, 1972.

3. Roskam, J., Lan, C., and Mehrotra, S.; "Method for Computing the Aerodynamic Influence Coefficient Matrix of Nonplanar Wing-Body-Tail Configurations," NASA CR-12231; Prepared under NASA Grant NGR 17-002-071 by the Flight Research Laboratory of the Department of Aerospace Engineering of the University of Kansas, October, 1972. Appendix C of the Summary Report, NASA CR-2117.